The Plant Cell, Vol. 16, 60–73, January 2004, www.plantcell.org © 2003 American Society of Plant Biologists

Programmed Cell Death Remodels Lace Plant Leaf Shape during Development[W]

Arunika H. L. A. N. Gunawardena,[a,b] John S. Greenwood,[c] and Nancy G. Dengler[a,1]

[a] Department of Botany, University of Toronto, Toronto, Ontario, Canada M5S 1A1
[b] Department of Agricultural Biology, Faculty of Agriculture, University of Peradeniya, Sri Lanka
[c] Department of Botany, University of Guelph, Guelph, Ontario, Canada N1G 2W1

Programmed cell death (PCD) functions in the developmental remodeling of leaf shape in higher plants, a process analogous to digit formation in the vertebrate limb. In this study, we provide a cytological characterization of the time course of events as PCD remodels young expanding leaves of the lace plant. Tonoplast rupture is the first PCD event in this system, indicated by alterations in cytoplasmic streaming, loss of anthocyanin color, and ultrastructural appearance. Nuclei become terminal deoxynucleotidyl transferase–mediated dUTP nick end labeling positive soon afterward but do not become morphologically altered until late stages of PCD. Genomic DNA is fragmented, but not into internucleosomal units. Other cytoplasmic changes, such as shrinkage and degradation of organelles, occur later. This form of PCD resembles tracheary element differentiation in cytological execution but requires unique developmental regulation so that discrete panels of tissue located equidistantly between veins undergo PCD while surrounding cells do not.

The Plant Cell

INTRODUCTION

Programmed cell death (PCD) is a genetically encoded, active process that results in the death of individual cells, tissues, or whole organs. Plants use the PCD process as one of many mechanisms that are required for the normal developmental elaboration of the plant life cycle. Developmental uses of PCD include (1) differentiation of specialized cell types such as tracheary elements, (2) deletion of tissues with ephemeral functions, such as the embryonic suspensor, and (3) organ or shoot morphogenesis, such as the formation of functionally unisexual flowers from bisexual floral primordia (Greenberg, 1996; Jones and Dangl, 1996; Beers, 1997; Pennell and Lamb, 1997; Jones, 2000, 2001; Kuriyama and Fukuda, 2002). Although the primary signals that initiate the PCD pathway have not been identified for any of these cases, they are presumably internal and respond to positional and temporal cues elaborated during plant development. By contrast, environmentally induced PCD, such as the development of lysigenous aerenchyma triggered by hypoxic stress (Gunawardena et al., 2001a, 2001b) and the hypersensitive response triggered by pathogen invasion (Ryerson and Heath, 1996; Mittler and Lam, 1997; Heath, 2000), is initiated in response to abiotic or biotic external signals.

The formation of complex leaf shape is a unique and fascinating use of developmental PCD. In a vast majority of vascular plants, pinnately or palmately dissected leaves are formed through localized growth enhancement or suppression during the early morphogenetic phase of leaf development (Kaplan, 1984; Sinha, 1999; Dengler and Tsukaya, 2001; Gleissberg, 2002). By contrast, the complex leaf shapes of a handful of monocotyledonous species arise solely through the death of discrete patches of cells early in the leaf expansion phase (Melville and Wrigley, 1969; Kaplan, 1984; Greenberg, 1996; Jones and Dangl, 1996; Beers, 1997; Pennell and Lamb, 1997). In certain *Monstera* species, the initial pinprick-sized holes formed by PCD are stretched by leaf expansion, and patches formed earlier tear through the leaf margin, forming a deeply lobed leaf (Melville and Wrigley, 1969; Kaplan, 1984). A single species of the aponogeton family, lace plant, uses PCD during leaf development in quite a different way (Sergueff, 1907): leaf blades retain a simple oblong outline during expansion but become perforated with rectangular holes that are positioned equidistantly between longitudinal and transverse veins. In both *Monstera* and lace plant, a discrete subpopulation of epidermal and mesophyll cells undergo PCD, whereas in adjacent, apparently identical tissues, PCD is not initiated. Although it is possible that developing leaf veins provide a positional signal for the initiation of cell death in these patches, nothing is known about the developmental cues, signaling pathways, or execution of cell death in these unique cases of developmental PCD.

PCD in plants encompasses a diverse set of mechanisms for the initiating trigger, signaling pathways, and cell death itself (Jones and Dangl, 1996; Fukuda, 2000; Jones, 2001; Hoeberichts and Woltering, 2002; Kuriyama and Fukuda, 2002). For instance, at least three major cytological variants of the PCD process are well characterized in plants (Fukuda, 2000). In apoptosis-like cell death, the nucleus is the first target of degradation, and dying cells exhibit characteristic features such as chromatin condensation, nuclear shrinkage and fragmentation, and DNA laddering (Fukuda, 2000). Cell death is rapid, and the degradation of organelles may be incomplete. By contrast, cell death associated with senescence typically proceeds slowly (Fukuda, 2000). In this form, chloroplasts are degraded first, allowing for high recovery of the breakdown products of enzymes and pigments, and disruption of the vacuole and nucleus occurs late,

[1] To whom correspondence should be addressed. E-mail dengler@botany.utoronto.ca; fax 416-978-5878.
[W] Online version contains Web-only data.
Article, publication date, and citation information can be found at www.plantcell.org/cgi/doi/10.1105/tpc.016188.

after the conversion of chloroplasts to gerontoplasts (Simeonova et al., 2000; Thomas et al., 2003). The early disruption of the large central vacuole characterizes the third cytological variant of PCD (Fukuda, 2000). In this form, the vacuole sequesters lytic enzymes such as nucleases and proteases that are released suddenly, acidifying the cytoplasm and rapidly degrading the nucleus and nucleoids of chloroplasts (Groover et al., 1997; Obara et al., 2001; Ito and Fukuda, 2002). The vacuolar collapse form of PCD is best characterized by the differentiation of tracheary elements but also has been observed during the postgerminative developmental PCD of wheat aleurone tissue (Kuo et al., 1996) and in response to pathogens (Mittler and Lam, 1997). Because the large central vacuole is a distinguishing feature of almost all plant cells, vacuolar collapse has been hypothesized to be common to all forms of plant PCD (Fukuda, 2000; Jones, 2001). Despite the differences in the execution of PCD at the cytological level and in the initiating triggers, there still may be commonalities in the signaling pathways that lead to PCD in plants and even functional conservation of some of these steps between plants and animals (Jones and Dangl, 1996; Fukuda, 2000; Jones, 2001; Hoeberichts and Woltering, 2002; Kuriyama and Fukuda, 2002).

In this study, light microscopy of living leaves and scanning and transmission electron microscopy of fixed tissues were used to characterize the development from an initial simple leaf shape to a final highly complex shape as PCD remodels young expanding leaves of lace plant. Video imaging was used to follow cytoplasmic streaming during the early stages of PCD, and whole-mount terminal deoxynucleotidyl transferase–mediated dUTP nick end labeling (TUNEL) assays and electrophoresis of isolated DNA were used to determine the timing of nuclear degradation in relation to other cytological events. The disruption of cytoplasmic streaming and the loss of anthocyanin, indicators of tonoplast disintegration, are the first signs of PCD and are followed closely by the appearance of TUNEL-positive nuclei. Although the cytological events resemble those seen during tracheary element differentiation, cell walls also must be degraded as part of the PCD process, thus providing the open "windows" of a mature lace plant leaf. Such an unusual use of developmental PCD in plants raises many intriguing questions. What cues trigger PCD at the appropriate stage of leaf development? How is a small patch of cells designated for the PCD pathway, whereas adjacent cells do not initiate PCD? What processes from signaling pathways and cell death mechanisms already present in ancestral aponogetons have been coopted for this purpose? Although *Monstera* and other aroids are more familiar examples of the involvement of PCD during leaf morphogenesis, they are much less tractable than lace plant, because perforations are formed while leaves are rolled tightly in the bud (Melville and Wrigley, 1969; Kaplan, 1984). The accessibility and predictability of leaf perforation formation in the aquatic lace plant provides an attractive model system for the study of developmental PCD in planta.

RESULTS

Perforation Formation during Leaf Development

Lace plant grows as a submerged aquatic, with leaves borne in subopposite pairs at the apex of a short spherical corm (Figure 1A). Mature leaves are fenestrate, with perforations resulting in a lattice pattern between the intersections of the seven longitudinal and numerous transverse veins (Figures 1A to 1C). Mature perforations are large and rectangular near the midvein and smaller and more rounded near the margin (Figure 1C). Immature leaves in the buds are rolled longitudinally and begin to unfurl when they reach a length of ~1.5 cm, ~10% of mature length. Young leaves are red as a result of anthocyanin (Figure 1D), and perforations are formed close to the midvein first and near the margin last.

Based on light microscopic and scanning electron microscopic observations of whole blade tissue, the continuous process of perforation formation was subdivided into five stages for convenience.

Stage 1: Preperforation

Leaves are still rolled longitudinally, but the vein pattern is complete (Figures 2A and 2B). The leaf lamina between veins is only

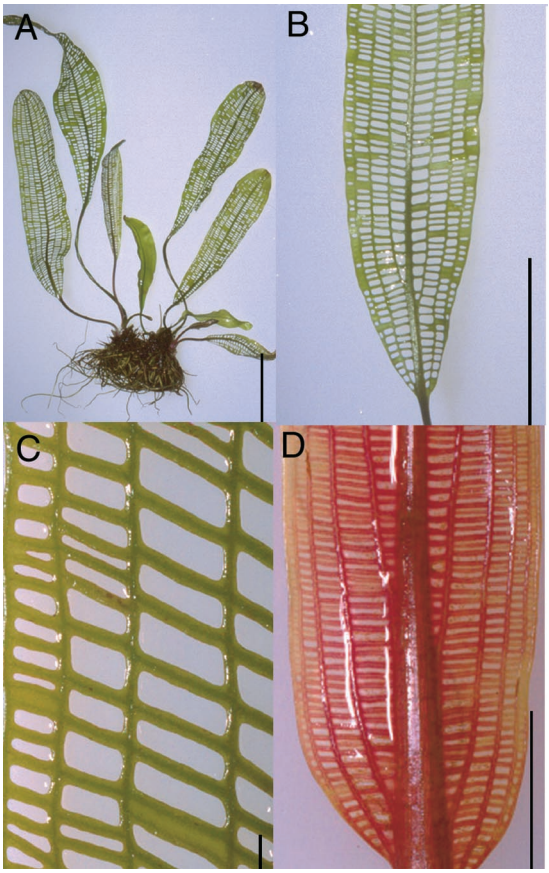

Figure 1. Morphology of Mature and Developing Leaves of Lace Plant.

(A) Whole plant.
(B) and **(C)** Mature leaf illustrating perforations between longitudinal and transverse veins.
(D) Immature leaf (stage 2) before perforation formation.
Bars = 5 cm in **(A)**, 3 cm in **(B)**, 1 mm in **(C)**, and 1 cm in **(D)**.

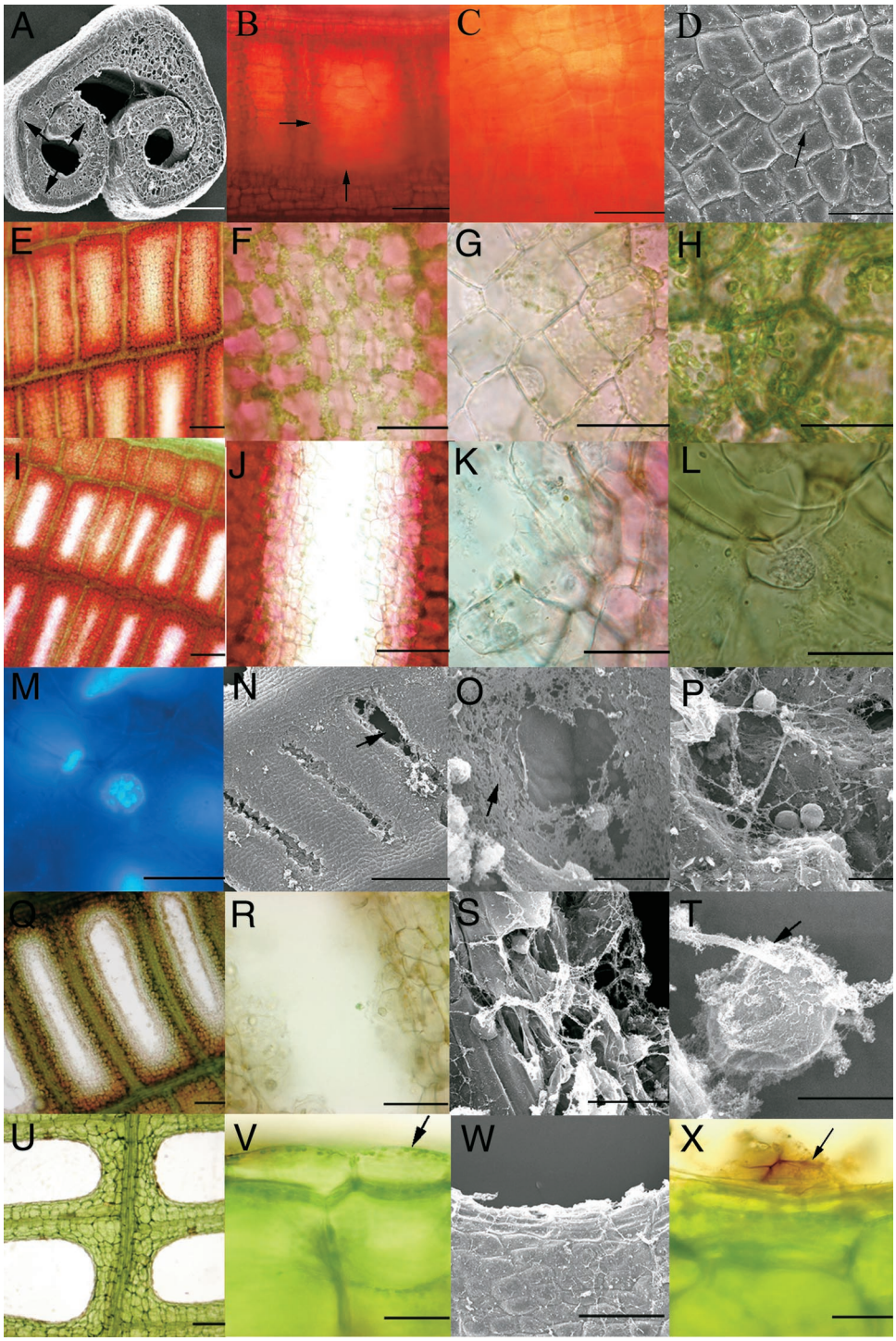

Figure 2. Light Micrographs of Living Leaves and Scanning Electron Micrographs of Fixed Tissue Illustrating the Stages of Perforation Formation in Lace Plant.

(A) to **(D)** Stage-1 leaves are rolled longitudinally, with no indication of perforation formation. The longitudinal and transverse vein pattern is complete (arrows in **[A]** and **[B]**). **(C)** shows that epidermal and mesophyll cells accumulate anthocyanin, and **(D)** shows shallowly indented anticlinal walls (arrow), indicating recent cell divisions in the epidermal layer.

(E) to **(H)** In stage 2, the first cells to initiate PCD at the center of the perforation site appear transparent as a result of the loss of anthocyanin and chlorophyll. **(H)** shows that mesophyll cells adjacent to veins retain pigments.

four cell layers thick (Tomlinson, 1982) (Figure 3A) and appears lighter than the thicker vein regions in living leaves. Epidermal cells, as well as mesophyll cells, contain chloroplasts, as is common in aquatic plants (Sculthorpe, 1967) (see supplemental data online). Both cell types also accumulate vacuolar anthocyanin (Figure 2C). Shallow surface indentations seen in scanning electron micrographs reflect newly formed anticlinal walls, indicating that cells in the epidermis are undergoing division at this stage (Figure 2D).

Stage 2: "Window" Formation

In newly unfurled leaves, distinct transparent regions appear between longitudinal and transverse veins as a result of the loss of anthocyanin and chlorophyll in epidermal and mesophyll layers (Figures 2E to 2G and 3B). By contrast, epidermal and mesophyll cells near the veins retain plastid chlorophyll and vacuolar anthocyanin (Figure 2H).

Stage 3: Perforation Formation

Cells at the center of the perforation site undergo degradation, opening the perforations first near the midvein and then toward the leaf margin (Figures 2I and 2N). In sectional view, epidermal and mesophyll cells appear to degrade simultaneously (Figure 3C), but in surface view, degradation of the outer tangential epidermal cell wall is the first externally visible indication of perforation (Figures 2N and 2O). As the perforation opens, cellular debris and intact nuclei (as indicated by 4′,6-diamidino-2-phenylindole staining) remain at the perforation border (Figures 2J to 2M and 2P). By contrast, mesophyll and epidermal cells at the border of the perforation appear normal (Figure 3C).

Stage 4: Perforation Expansion

Leaf expansion increases the size of individual perforations by ~10-fold. Dying cells rim the border of the perforation, leaving remnants of cell walls, cytoplasmic debris, and nuclei (Figures 2Q to 2T and 3D).

Stage 5: Mature Perforation

Leaf expansion and perforation formation are complete at this stage (Figures 2U to 2X and 3F). Living cells at the border of the perforation form a continuous surface (Figure 2V), although cell wall remnants impregnated with brown phenolic substances persist at the perforation edge (Figures 2W and 2X).

Transdifferentiation of Mesophyll Cells

Two layers of mesophyll cells are exposed at the perforation margin during stages 3 and 4 (Figures 3C and 3D). These cells retain a narrow diameter and do not undergo the cell enlargement that characterizes other cells in these two internal layers during stage-4 leaf expansion (Figure 3E). Because of their position at the perforation margin, these cells maintain the continuity of the layer of living epidermal cells at the surface of the mature leaf (Figure 3F). During stage-4 expansion, these mesophyll-derived cells adopt the narrow, elongate shape of epidermal cells (Figures 2V, 3G, and 3H).

DNA Cleavage during Perforation Formation

Cleavage of nuclear DNA during perforation formation was followed using the TUNEL assay on whole-mount tissue samples. Stage-1 leaves lack TUNEL-positive nuclei (data not shown). At stage 2, TUNEL-positive nuclei are present in a rectangular zone at the center of the future perforation site (Figures 4A to 4D). Propidium iodide staining identifies these nuclei, as well as TUNEL-negative nuclei in surrounding tissue (Figures 4B to 4D). At stage 3, TUNEL-positive nuclei are present in a broader zone of tissue, with gaps where the perforation has broken through all four cell layers (Figures 4E to 4G). At stage 4, a zone of TUNEL-positive nuclei extends continuously around the border of the perforation for most of the period of leaf expansion (Figures 4H to 4M). At stage 5, no TUNEL-positive nuclei are observed in leaf tissues (Figures 4N to 4Q).

Genomic DNA was isolated from leaves at stages 2 to 5 and separated by agarose gel electrophoresis (Figure 5). At stage 2 (lane 2), extensive DNA smearing is detected, indicating degradation of DNA. Decreasing amounts of smearing are observed at stages 3 to 5. However, there is no obvious "laddering" of DNA degradation of the genomic DNA into internucleosomal fragments of multiples of ~180 bp.

Early Disruption of Cytoplasmic Streaming

Cytoplasmic streaming is a conspicuous feature of plant cell behavior in which organelles and vesicles shuttle along cyto-

---

Figure 2. (continued).

(I) to **(P)** In stage 3, degradation of the first cells to undergo PCD forms an opening at the center of the perforation site (**[I]** to **[K]**). In **(L)**, **(M)**, and **(P)**, cellular debris, including intact nuclei, remain at the perforation margin. **(L)** shows a nucleus viewed with differential interference contrast optics. **(M)** shows the same nucleus stained with 4′,6-diamidino-2-phenylindole. **(N)** to **(P)** show scanning electron micrographs of early perforation formation. Some perforations extend through lamina (arrow in **[N]**), whereas others are incomplete. **(O)** shows the early stage of epidermal cell wall degradation (arrow), and **(P)** shows intact nuclei after degradation of the epidermal layer.

(Q) to **(T)** During stage 4, perforations enlarge as the leaf expands. Cellular debris and intact nuclei (arrow) are seen at the perforation margin.

(U) to **(X)** Stage-5 (mature) leaves. **(V)** and **(W)** show that mesophyll cells at the perforation margin have transdifferentiated as elongate epidermal cells (arrow). **(X)** shows that remnants of cell walls at the perforation margin are impregnated with brown phenolic compounds (arrow).

Bars = 250 μm in **(A)** and **(N)**, 150 μm in **(B)**, **(E)**, **(I)**, **(Q)**, **(U)**, and **(W)**, 50 μm in **(C)**, **(F)**, **(J)**, **(R)**, **(S)**, **(V)**, and **(X)**, 25 μm in **(D)**, **(G)**, **(H)**, **(K)**, **(L)**, and **(M)**, and 5 μm in **(O)**, **(P)**, and **(T)**.

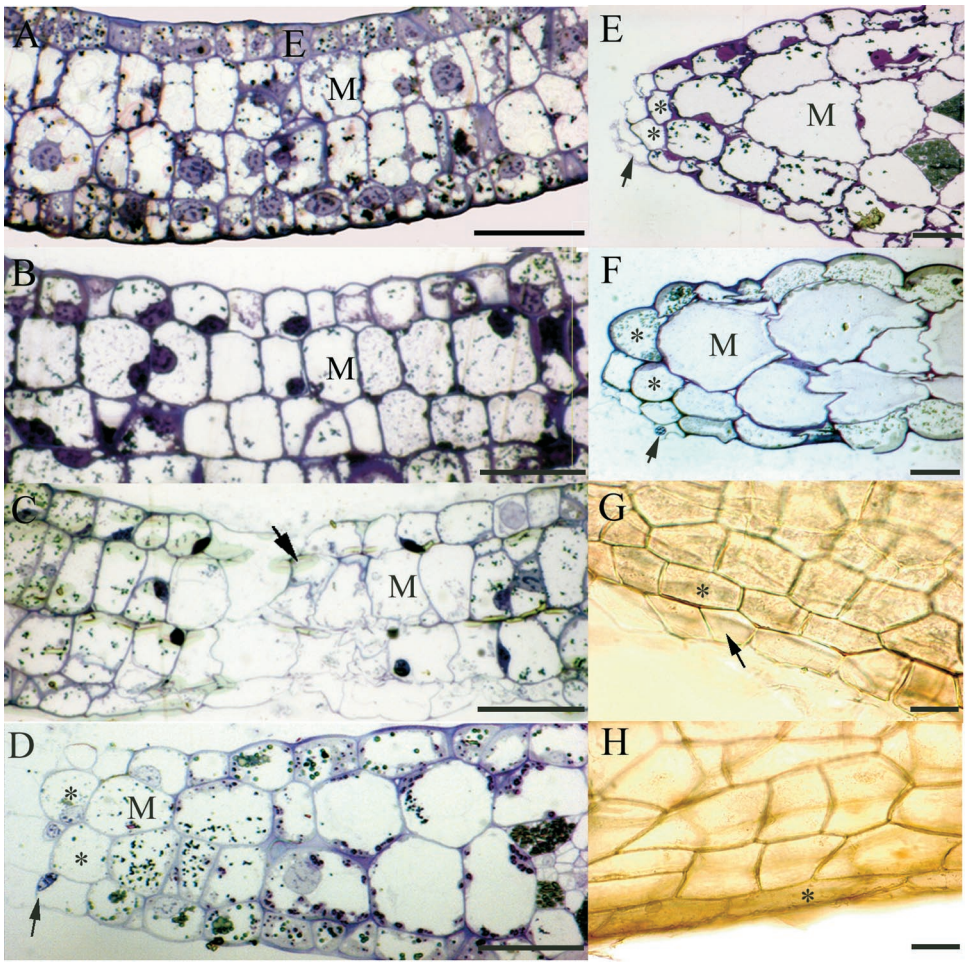

Figure 3. Light Micrographs of Spurr-Embedded Tissues Stained with Toluidine Blue O and of Unstained Cleared Tissues Showing the Five Stages of Perforation Formation and the Properties of Transdifferentiating Cells.

(A) Stage 1. Epidermal and mesophyll layers at perforation site between veins.
(B) Stage 2. Cells in both epidermal and mesophyll layers are vacuolated.
(C) Stage 3. Degradation of epidermal and mesophyll cells at the center of the perforation (arrow).
(D) Stage 4 (early). Living cells (asterisks) and dying cells (arrow) at the perforation margin.
(E) Stage 4 (late). Enlargement of mesophyll cells, except those at the perforation margin (asterisks). Note the remnants of dead cells (arrow) and the continuity of the living surface layer.
(F) Stage 5 (mature). Perforation margin with small-diameter epidermal cells (asterisks) and remnants of dead cells (arrow).
(G) Stage 4. Clearing focused at the mesophyll layer. A living future epidermal cell of the perforation margin (asterisk) and an adjacent dead cell (arrow) are seen.
(H) Stage 5. Clearing showing the shape of a transdifferentiated cell (asterisk).
E, epidermis; M, mesophyll. Bars = 50 μm.

plasmic strands. Active directed cytoplasmic streaming is a hallmark of healthy living cells; thus, alteration of cytoplasmic streaming is predicted to be an early indicator of cell death. Video imaging of epidermal and mesophyll cells adjacent to vascular bundles (control tissue) revealed normal cytoplasmic streaming with prominent movement of mitochondria and chloroplasts (Figure 6A; see also supplemental data online). The same results were observed in leaves taken at stage 1 (early and mid), although clear imaging was not possible because of the density of the cytoplasm. At late stage 1 and early stage 2, cells at the center of the perforation site display more rapid, erratic, nondirected movement of cytoplasmic and/or vacuolar contents, in contrast to the control cells in the perforation border (Figure 6B; see also supplemental data online). At stage 3, a gradient is observed between control cells at the perforation border with anthocyanin and actively streaming chloroplasts (Figure 6D) and cells at the perforation center in which streaming had ceased (Figures 6E to 6G); this gradient is interpreted to represent progressive stages of cell death. Cells first lose anthocyanin and individual plastids appear smaller (Figure 6E).

These cells show more rapid, erratic, nondirected cytoplasmic streaming. Later, a loss of plastids is observed (Figure 6F). Finally, all streaming ceases (see supplemental data online), followed by cytoplasmic collapse (Figures 6C and 6G; see also supplemental data online).

Cell Ultrastructure during PCD

Epidermal and mesophyll cells from stage-1 leaves are vacuolate, with large, rounded nuclei (Figures 7A to 7F). Condensed chromatin is distributed throughout the nucleus. Vacuoles contain electron-dense bodies, possibly polyphosphate granules. Chloroplasts and mitochondria are conspicuous, and the plasma membrane and tonoplast are intact. The first signs of PCD are observed early in stage 2 (Figures 7G to 7L). Both epidermal and mesophyll cells have a thin layer of peripheral cytoplasm. At first, the tonoplast invaginates, appearing to pinch off vesicles into the vacuole (Figure 7H). With progression through the PCD process, elaborate membrane systems and vesicles appear in the vacuolar space (Figure 7I, both cells), and the tonoplast becomes difficult to distinguish (Figure 7I, left cell). Nuclei still possess intact nuclear envelopes and increasing amounts of condensed chromatin (Figure 7J). The plasma membrane remains appressed to the cell wall. Chloroplasts are intact (Figure 7K), but thylakoid membranes are less conspicuous compared with those seen in adjacent control tissue (Figure 7L). By late stage 2, cellular ultrastructure is highly disrupted (Figures 8A to 8F). The plasma membrane is retracted from the cell wall. Nuclei are intact, with much condensed chromatin, and may be either round or lobed in outline (Figures 8D and 8E). Peripheral cytoplasm is diffuse and contains vesicles and some intact, but misshapen, organelles (Figure 8F).

Stage 3 is defined by the perforation breaking through from one side of the lamina to the other. Thin and broken cell walls are apparent in light and electron micrographs (Figures 3C and 8G). Although nuclei are present as discrete bodies, chromatin appears completely condensed and the remaining nucleoplasm is electron transparent (Figure 8H). Degraded organelles and other remnants of cytoplasmic components remain in some cells at this stage (Figure 8I). By contrast, epidermal and mesophyll tissues near veins are composed of healthy cells with intact vacuoles, plasma membranes, nuclei, and organelles all with normal appearance (Figures 8J to 8L).

DISCUSSION

PCD Remodels Leaf Shape

In a process analogous to digit formation in vertebrates, leaf shape in the lace plant is remodeled by PCD. An initially simple leaf blade is resculpted to form an open lattice, with each bar consisting of a centrally placed vein surrounded by a few layers of mesophyll and the epidermal layers. PCD occurs in discrete linear patches that are positioned equidistantly between the longitudinal and transverse veins. Cytoplasm, nuclei, and cell walls are degraded so that the initial interveinal fenestration opens as the leaf blade expands. Additional cells undergo PCD, so that the expanding perforation is lined with dying cells. Cell wall degradation often is not complete for these late dying cells, and cell wall remnants persist, lining the perforation in mature leaves. Living mesophyll cells at the perforation boundary transdifferentiate into epidermal cells, so that each perforation is bounded by a continuous layer of elongate epidermal cells. Such a remodeling of leaf shape is known only for lace plant and a handful of species of *Monstera* and related aroid genera (Melville and Wrigley, 1969; Madison, 1977; Kaplan, 1984). The use of PCD in leaf morphogenesis in these two distantly related groups of monocots is a striking example of evolutionary convergence and provides a unique opportunity to study how the cellular mechanisms of PCD present in the ancestors of these groups might have been recruited for this unique purpose.

Vacuolar Collapse Precedes Nuclear Degradation

Although this unusual mode of leaf morphogenesis was first described more than a century ago (Trècul, 1854; Sergueff, 1907), the cellular and molecular mechanisms associated with this unique function of PCD are completely unknown. In this study, the cytological events of PCD during leaf shape remodeling in lace plant were characterized using light microscopy and video imaging of living tissues and scanning and transmission electron microscopy of fixed leaves. Both whole-mount TUNEL assays and electrophoresis of isolated DNA were used to analyze the degradation of genomic DNA during the PCD process.

Based on our observations, we hypothesize that alteration of tonoplast permeability/rupture is the first structural event of PCD during leaf remodeling. Both the rapid alteration of cytoplasmic streaming and the disappearance of anthocyanin pigment, occurring in late stage 1 and early in stage 2, suggest a loss of tonoplast integrity and a mixing of acidic vacuolar contents with the cytoplasm. The more rapid, erratic, nondirected movement of large particles within the cell before streaming ceases might reflect the coagulation of cytoplasmic components or the alteration of the physical properties of the cytosol as a result of acidification. Early tonoplast disruption also is suggested by the ultrastructural appearance of invaginations of the tonoplast membrane and numerous vesicles within the vacuolar space.

The sequence of events during the formation of lace plant leaf perforations is similar to that observed during the differentiation of tracheary elements from cultured zinnia mesophyll cells (Mittler and Lam, 1995; Groover et al., 1997; Fukuda, 2000; Obara et al., 2001). In the zinnia system, PCD proceeds rapidly: once initiated, the loss of tonoplast selective permeability, vacuolar collapse, and cessation of cytoplasmic streaming are followed by the degradation of nuclear and organellar DNA within 15 to 20 min (Groover et al., 1997; Kuriyama, 1999; Obara et al., 2001). Similarly, vacuolar collapse precedes DNA degradation in lace plant, as shown by whole-mount TUNEL assays and by electrophoresis of isolated DNA. Although a lack of detailed knowledge of the sequence of cytological events makes comparison across functional categories of PCD difficult, the collapse of the large lytic central vacuole is a feature common to many forms of plant PCD (Jones, 2001). For instance, cessation of cytoplasmic streaming and/or tonoplast rupture are among the first responses to invasion by some pathogens (Mittler et al., 1997; Heath, 2000) and in the formation of aerenchyma in response

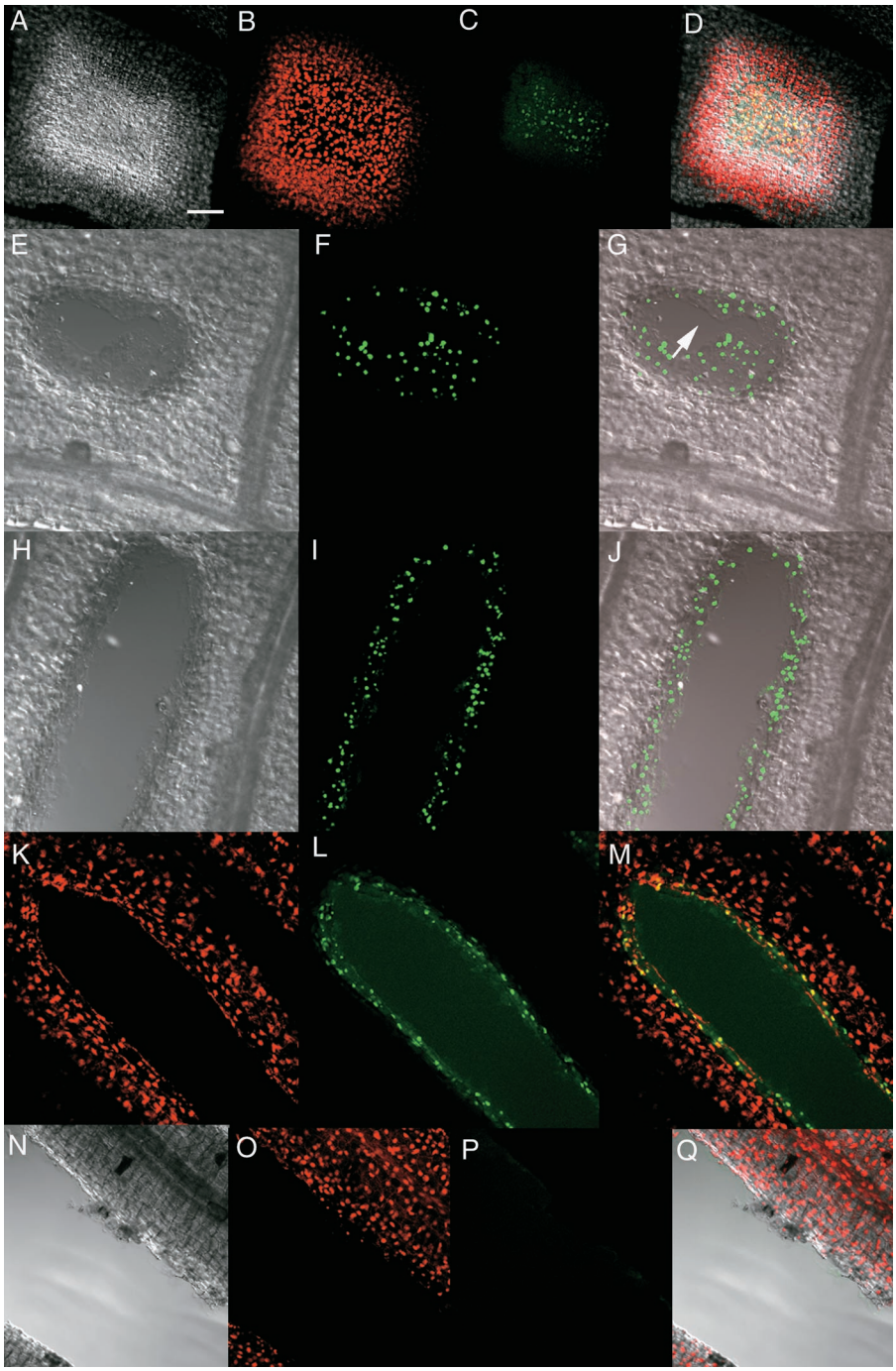

Figure 4. Confocal Microscopy and Differential Interference Contrast Microscopy Showing Detection of DNA Cleavage by TUNEL Assay.

(A) to **(D)** Stage-2 (window) perforation site.
(A) Differential interference contrast (DIC) image.
(B) Confocal microscopy (CM) image of propidium iodide–stained nuclei indicated by red fluorescence.
(C) TUNEL-positive nuclei indicated by green fluorescence at the center of the site.
(D) Merged image of **(A)** to **(C)**.
(E) to **(G)** Stage-3 (perforation formation) perforation site.
(E) DIC image.
(F) CM image of TUNEL-positive nuclei indicated by green fluorescence.
(G) Merged image of **(E)** and **(F)**. Perforation extends through the leaf lamina (arrow).

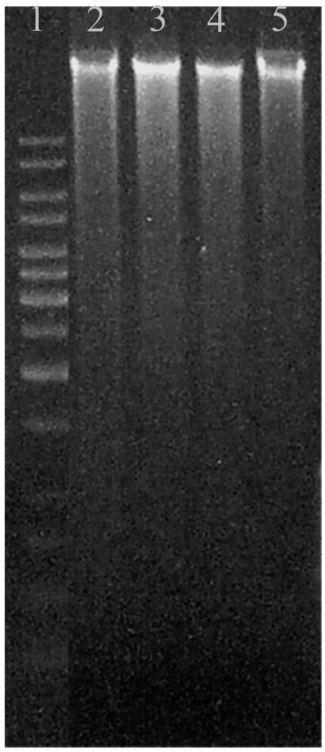

Figure 5. DNA Cleavage in Developing Leaves.

Lane 1, molecular mass markers (100 bp). Lanes 2 to 5, genomic DNA isolated from developing leaves taken at stage 2 (lane 2), stage 3 (lane 3), and stage 4 (lane 4) and from mature leaves (lane 5), stained with ethidium bromide, and separated electrophoretically. Extensive DNA smearing was present, indicating the degradation of DNA without laddering into internucleosomal fragments of ~180 bp at stage 2 (lane 2). DNA smearing is reduced at stages 3 (lane 3) and 4 (lane 4). Only limited DNA smearing occurs at stage 5 (lane 5).

to hypoxia (Campbell and Drew, 1983; Gunawardena et al., 2001a).

Cleavage of genomic DNA into smaller fragments is a hallmark of PCD. In animal apoptosis, DNA is first cleaved into large fragments of 50 to 300 kb (Wyllie et al., 1980; Oberhammer et al., 1993). Subsequently, DNA is cleaved at internucleosomal linker regions, producing fragments that are multimers of ~180 bp, identified by a ladder-like pattern when separated electrophoretically. Finally, the fragmented DNA is digested completely by specific endonucleases. Although electrophoresis can provide evidence for this specific pattern of DNA fragmentation, it cannot demonstrate tissue or cell specificity in planta. Furthermore, DNA laddering is difficult to demonstrate electrophoretically in extracts from tissues in which only a fraction of the cells are undergoing the fragmentation process (Wang et al., 1996). Therefore, a combination of electrophoresis of isolated DNA and the TUNEL assay was used to identify lace plant nuclei that were undergoing DNA fragmentation. Nuclei became TUNEL positive soon after tonoplast rupture and persisted until the very late stages of PCD in the sites of perforation formation. DNA laddering was not observed at any stage of perforation formation. Rather, extensive smearing, indicating DNA fragments of a continuous size range, was observed after electrophoresis of DNA from tissues with TUNEL-positive nuclei.

Although DNA degradation produces both TUNEL-positive nuclei and DNA laddering in many forms of plant PCD, including the hypersensitive response to pathogens (Ryerson and Heath, 1996), aerenchyma formation in response to hypoxic stress (Gunawardena et al., 2001a), and normal development in certain nucellus, scutellum, and anther tissues (Wang et al., 1999; Dominguez et al., 2001; Giuliani et al., 2002), cleavage into 180-bp multimers is not detected during the differentiation of tracheary elements (Mittler and Lam, 1995; Groover et al., 1997), in soybean cells in response to bacterial pathogens (Levine et al., 1996), or in barley aleurone protoplasts undergoing PCD (Fath et al., 1999), even though nuclei from comparable cells are TUNEL positive. These apparently contradictory results presumably reflect the diversity of pathways by which plant PCD is executed. For instance, increased activity of several kinds of nucleases have been identified during plant PCD (reviewed by Sugiyama et al., 2000). S1-type nucleases are restricted in plants, and one of these, *ZINNIA ENDONUCLEASE1* (*ZEN1*), has been shown to play a major role in nuclear degradation during tracheary element PCD (Ito and Fukuda, 2002). When *ZEN1* nuclease is incubated with cell extracts, a smear pattern of nuclear DNA degradation is pro-

Figure 4. (continued).

(H) to **(J)** Stage-4 perforation early in leaf expansion.
(H) DIC image.
(I) CM image of TUNEL-positive nuclei in a zone three to four cells wide at the margin of the perforation.
(J) Merged image of **(H)** and **(I)**.
(K) to **(M)** Stage-4 perforation late in leaf expansion.
(K) CM image of propidium iodide–stained nuclei.
(L) CM image of TUNEL-positive nuclei in a zone one to two cells wide at the margin of the perforation.
(M) Merged image of **(K)** and **(L)**.
(N) to **(Q)** Portion of a stage-5 perforation in a fully mature leaf.
(N) DIC image.
(O) CM image of propidium iodide–stained nuclei.
(P) CM image showing the absence of TUNEL-positive nuclei at the perforation margin.
(Q) Merged image of **(N)** to **(P)**.
Bar in **(A)** = 50 μm for all panels.

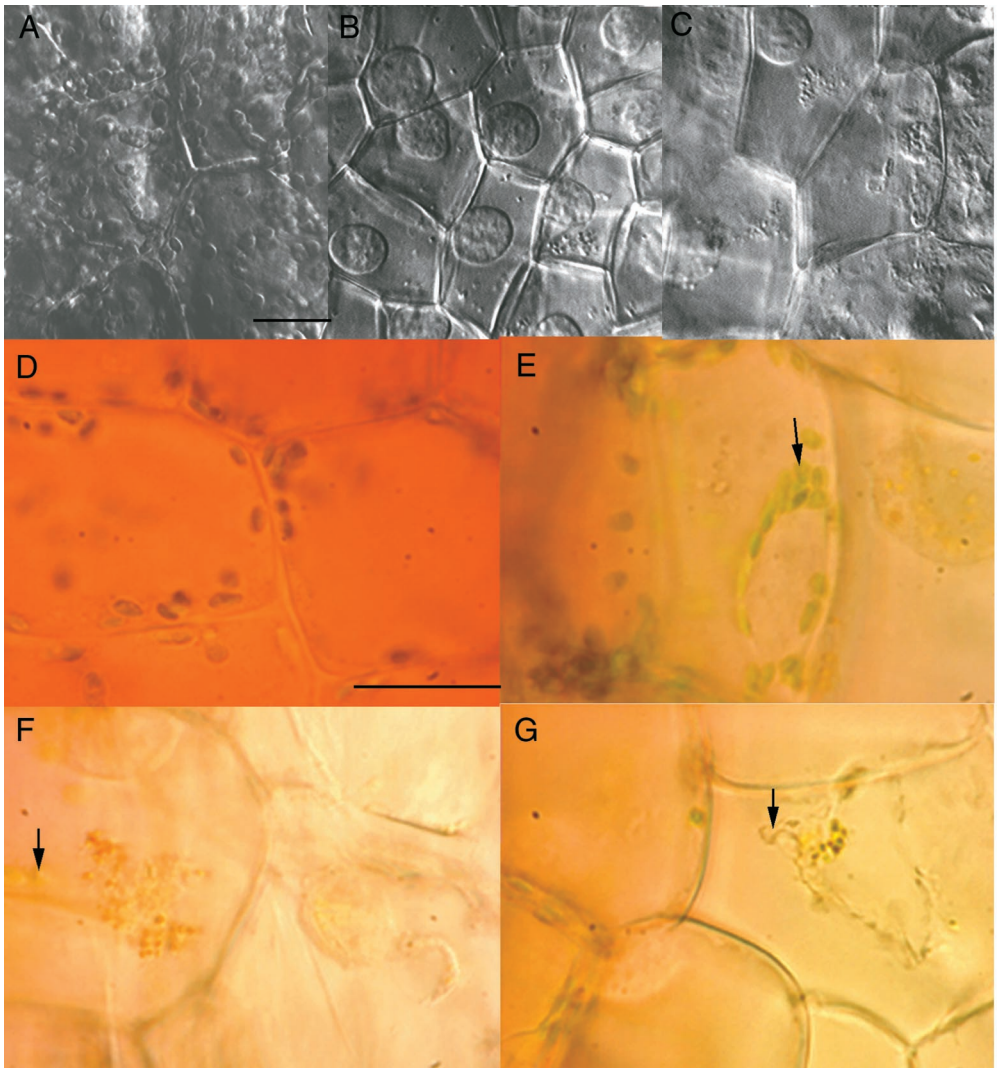

Figure 6. Light Micrographs Showing Changes in Cytoplasm during PCD.

(A) to **(C)** Still images from the beginning (**[A]**, stage 3, control tissue), middle (**[B]**, stage-2 perforation site), and end (**[C]**, stage-3 perforation site) of the video illustrating cytoplasmic streaming. Bar = 25 μm.
(D) to **(G)** Changes along the gradient from the vein to the center of the perforation site in a stage-3 leaf. Bar = 25 μm.
(D) Cells near the vein showing both anthocyanin and chloroplasts.
(E) Loss of anthocyanin, but chloroplasts (arrow) are present in cells at the outer periphery of the perforation site.
(F) Chloroplasts (arrow) are barely detectable.
(G) Collapse of cytoplasm (arrow).

duced, indicating that this particular nuclease differs from the conserved nuclear degradation machinery characteristic of many forms of animal apoptosis (Ito and Fukuda, 2002).

Degradation of Cytoplasm, Nucleus, and Cell Walls

After tonoplast disruption and the initiation of DNA degradation, the cytoplasm first becomes less dense and then shrinks, separating the plasma membrane from the cell wall. Plastids and mitochondria remain intact, but they are swollen and their internal membranes are disrupted. The nucleus looks remarkably normal, with condensed chromatin and an intact nuclear envelope, until late in the PCD process. It is only after the cytoplasmic density has been reduced and cell walls are disrupted that the nucleus displays an irregular shape, with an invaginated nuclear envelope and highly condensed, peripheral chromatin. This apoptosis-like nuclear morphology has been described in other forms of plant PCD, including aerenchyma formation in response to hypoxic stress (Gunawardena et al., 2001a) and the response of cultured BY-2 tobacco cells in response to oxidative stress (Houot et al., 2001). Although chromatin condensation has not been observed during tracheary element differ-

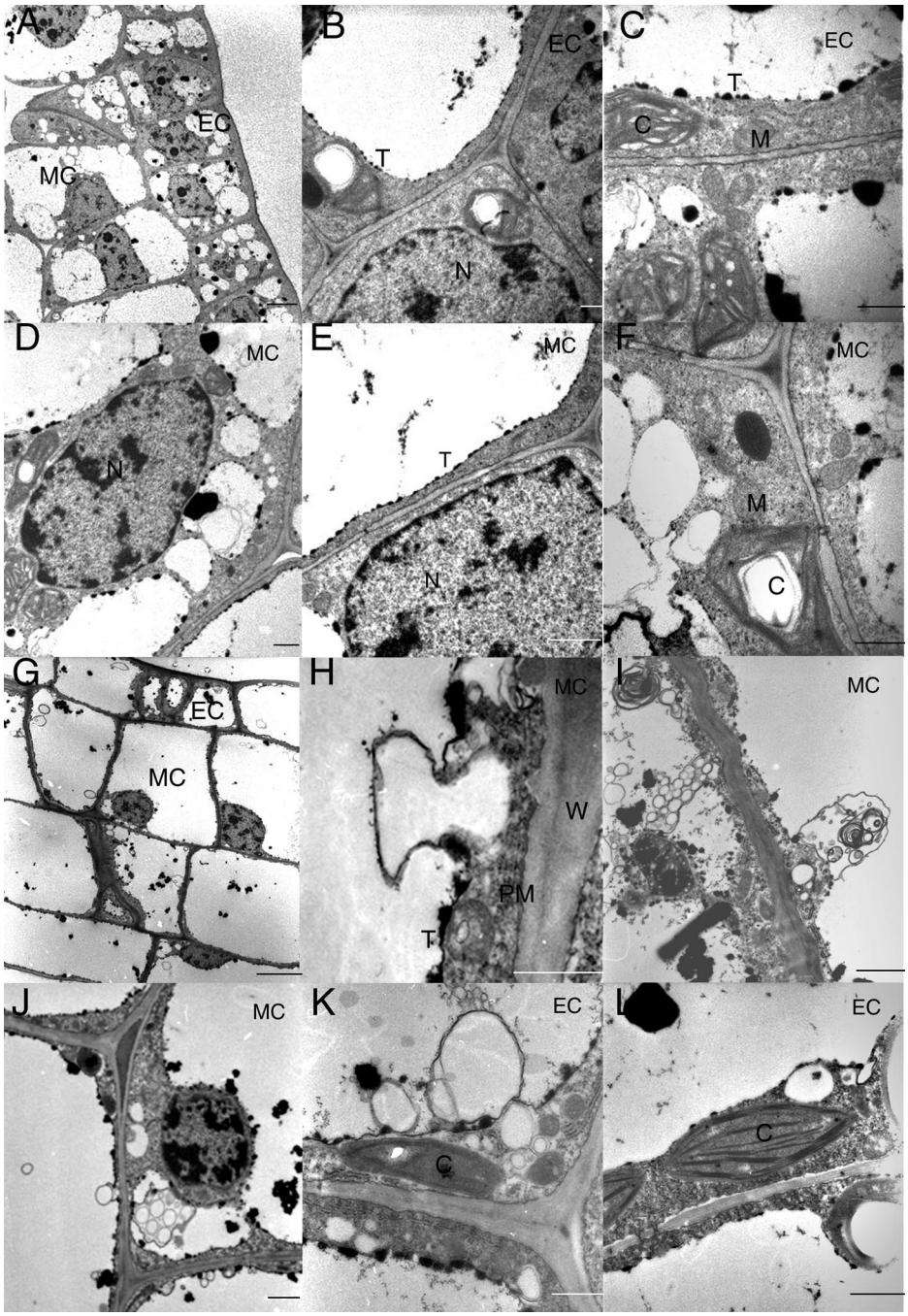

Figure 7. Transmission Electron Micrographs of Tissue from Perforation Sites and Adjacent Control Tissue at Stages 1 and 2.

(A) to **(F)** Stage-1 epidermal and mesophyll cells from a future perforation site. Epidermal cells (**[B]** and **[C]**) and mesophyll cells (**[D]** to **[F]**) showing intact vacuoles with tonoplast, nuclei, plasma membrane, chloroplasts, and mitochondria.

(G) to **(K)** Early stage-2 tissue from a perforation site showing invagination of the tonoplast membrane **(H)**, abundant vesicles and disintegration of the tonoplast **(I)**, intact nuclei **(J)**, and organelles **(K)**. The ultrastructure of epidermal cells **(K)** and mesophyll cells (**[H]** to **[J]**) is similar.

(L) An intact epidermal cell from adjacent control tissue.

C, chloroplast; EC, epidermal cell; M, mitochondrion; MC, mesophyll cell; N, nucleus; PM, plasma membrane; T, tonoplast; W, cell wall. Bars = 10 μm in **(A)** and **(G)** and 1 μm in **(B)** to **(F)** and **(H)** to **(L)**.

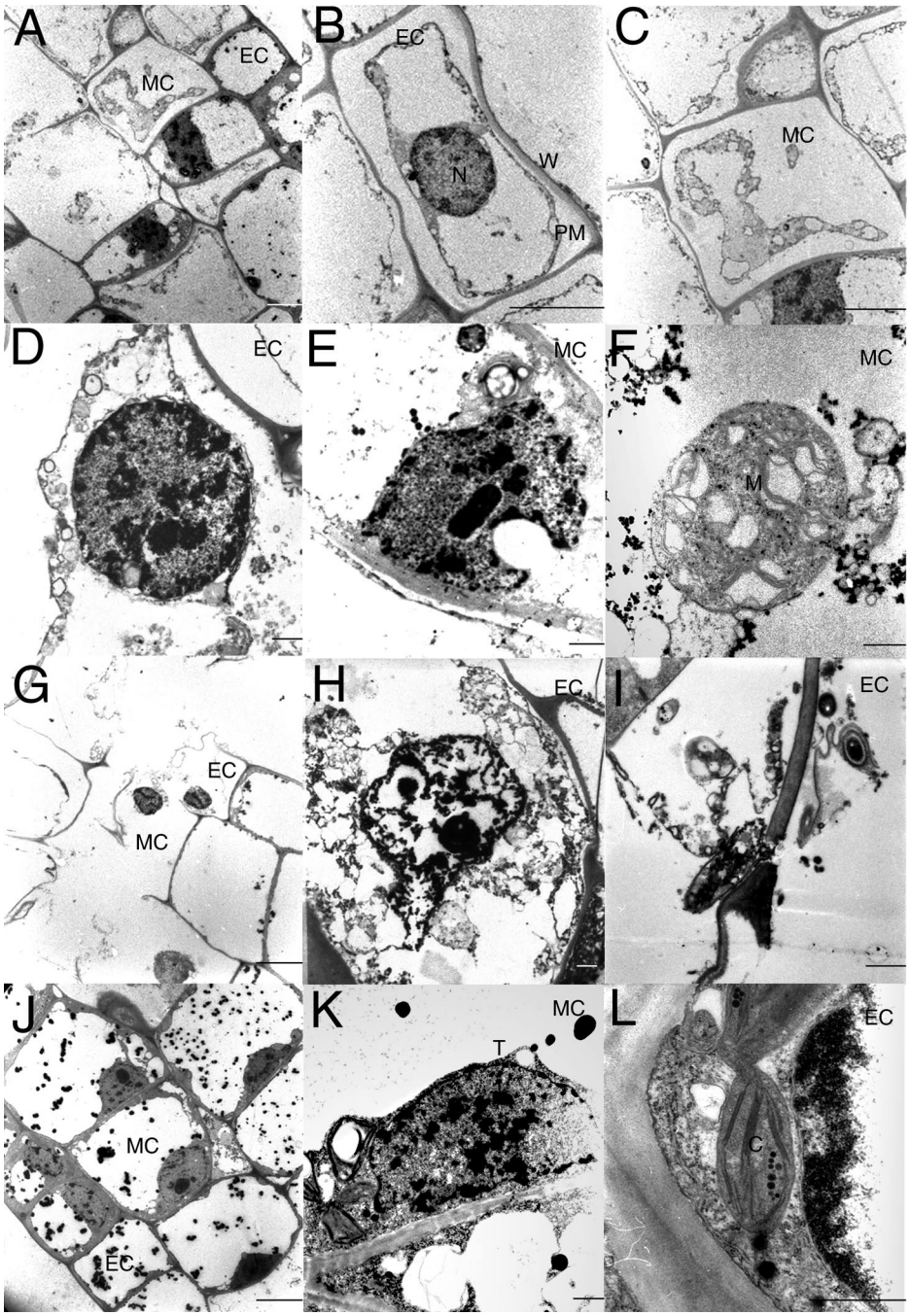

Figure 8. Transmission Electron Microscopy of Tissue from Perforation Sites and from Adjacent Control Tissue at Stages 2 and 3.

(A) to **(F)** Late stage-2 tissue showing retraction of the plasma membrane from the cell wall. Nuclei are intact, with well-distributed heterochromatin, but some are lobed **(E)**. Cytoplasm is diffuse and contains numerous vesicles and some recognizable organelles **(F)** in epidermal (**[B]** and **[D]**) and mesophyll (**[C]**, **[E]**, and **[F]**) cells.

(G) to **(I)** Stage-3 tissue from a perforation site. Cell walls are thin and disrupted, allowing perforation to break through the leaf lamina **(G)**. Chromatin is condensed, and nucleoplasm is thin **(H)**. Remnants of chloroplasts and other cytoplasmic components remain in some cells **(I)**.

(J) to **(L)** Stage-3 control tissue from a site adjacent to the perforation. All cells have large central vacuoles filled with a granular substance **(J)**. Nuclei have nucleoli, distributed condensed chromatin, and an intact nuclear envelope (**[J]** and **[K]**). Cytoplasm is dense, and the plasmalemma is appressed to the cell wall **(L)**.

C, chloroplast; EC, epidermal cell; M, mitochondrion; MC, mesophyll cell; N, nucleus; PM, plasma membrane; T, tonoplast; W, cell wall. Bars = 10 μm in **(A)** to **(C)** and **(J)** and 1 μm in **(D)** to **(I)**, **(K)**, and **(L)**.

entiation (Groover et al., 1997), cell death in this model system is rapid, and the stage may have been missed during ultrastructural analysis.

The plant cell wall may or may not be degraded along with the protoplast, depending on the type of PCD (Jones, 2001). During tracheary element differentiation, the primary wall and a rigid secondary wall are required for cell function and are not hydrolyzed, save for the portion of the primary wall between adjacent tracheary elements that is degraded to form a perforation (Nakashima et al., 2000). In most other forms of developmental PCD, collapsed primary cell walls are left behind, whereas nutrients from the dismantled protoplasts are recycled (Cheng et al., 1983; Young et al., 1997; He and Kermode, 2003). When the hypersensitive response is induced by pathogen invasion, the protoplast dies, leaving collapsed or crushed primary cell walls behind (Mittler et al., 1997). By contrast, cell walls must be degraded to form the extensive lysigenous air spaces in hypoxia-induced aerenchyma tissues in maize and rice roots (He et al., 1994; Gunawardena et al., 2001a, 2001b; Kozela and Regan, 2003). Based on the pitted appearance of lace plant cell walls in scanning electron micrographs and the thinned and broken appearance in light and electron micrographs, we hypothesize that cell wall degradation is an integral part of PCD during leaf perforation in lace plant.

Transdifferentiation of Mesophyll Cells

Transdifferentiation involves the conversion of a cell or tissue from one differentiated state to another (Thomas et al., 2003). In the zinnia culture system, isolated cells that were already differentiated as mesophyll cells first dedifferentiate, losing their capacity for photosynthesis, and then differentiate as tracheary elements in response to specific growth factors (Demura et al., 2002; Milioni et al., 2002). At the time of perforation formation, lace plant mesophyll cells have numerous chloroplasts and a large, anthocyanin-filled central vacuole, indicating that it is appropriate to regard them as differentiated, although they have not yet reached full size. The differentiation of these cells as epidermal cells is subtle compared with tracheary element differentiation, because there are few epidermis-specific anatomical markers in this aquatic species (a histochemically detectable cuticle layer is not present, and epidermal cells are as chloroplast rich as mesophyll cells). Nevertheless, mesophyll cells left exposed at the perforation margin follow a strikingly different pattern of cell expansion compared with their neighboring mesophyll cells: they become elongate, similar to adjacent epidermal cells, and form part of the continuous epidermis that lines the perforations.

Lace Plant as a Model System for Studying Plant PCD

PCD during leaf remodeling in lace plant is progressive: an initial narrow rectangular zone of cells positioned equidistantly from longitudinal and transverse veins dies in a synchronous manner. The zone of PCD spreads peripherally, with two to three more cell layers forming a gradient of progression through the PCD process, but then attenuates sharply, leaving a continuous border of living cells around the formed perforation. This pattern resembles other cases of developmental PCD in multicellular organs and tissues. For instance, in the abortion of stamen primordia in female flowers of maize, PCD begins near the apex of the primordium and then spreads basipetally, forming an abrupt border with living cells near the base of the original primordium (Cheng et al., 1983; Dellaporta and Calderon-Urrea, 1994; Calderon-Urrea and Dellaporta, 1999). In maize, the starchy endosperm tissue dies progressively from tip to base during seed development (Young et al., 1997), and in spruce, the functionally comparable megagametophyte also dies progressively, beginning near the embryonic radicle and spreading outward (He and Kermode, 2003). These consistent spatial and temporal patterns suggest a tight developmental control of PCD. Cell death is limited to specific whole tissues in endosperms, embryonic suspensors, scutella, and the megagametophyte, but in lace plant and the maize stamen primordia (Cheng et al., 1983), the abrupt boundary between living and dead cells forms across seemingly homogeneous tissues. Such a pattern might indicate that threshold levels of initiating signals do not reach these cells, or that they are not competent to respond, or that they are protected from the death-inducing signals (Jacobson et al., 1997; Calderon-Urrea and Dellaporta, 1999).

The precise placement of perforations equidistantly between veins in the leaves of lace plant (this study) and of *Monstera* (Melville and Wrigley, 1969) suggests that signals initiating PCD in more distal cells, or those that involve protection against the death of more proximal cells, may originate in the vascular tissues. This has been proposed for the placement of specialized cell types in the leaves of many higher plants (Nelson and Dengler, 1997). Although nothing is known about the signaling steps that lead to the cytological events described here, lace plant may provide a tractable system in which to study the putative intracellular movement of death-activating or death-suppressing molecules. For instance, the ability to perform the TUNEL assay on whole-mount tissue facilitates a spatial and temporal comparison of the expression of signaling genes with the events of PCD, much as has been done for the vertebrate limb (Grotewold and Rüther, 2002).

METHODS

Plant Material

Lace plant (*Aponogeton madagascariensis*) was supplied by Florida Aquatic Nurseries (Fort Lauderdale, FL) and maintained in 12-gallon aquaria in a growth chamber under 12-h-light/12-h-dark cycles at 20°C and 290 $\mu mol \cdot m^{-2} \cdot s^{-1}$ light at the University of Toronto. Expanding leaves were measured every 2 days to obtain growth curves ($n = 20$) and to determine developmental staging. Fresh leaves representing stages 1 to 5 were harvested at appropriate intervals. Tissue samples from living and cleared (in saturated chloral hydrate) leaves were examined by bright-field, differential interference contrast, or fluorescence microscopy using a Reichert-Jung Polyvar microscope (Vienna, Austria) and recorded using a Nikon DXM 1200 digital camera (Nikon Canada, Mississauga, Ontario).

Scanning Electron Microscopy

Tissue samples (5 mm^2) from leaves at developmental stages 1 to 5 were fixed in FAA (formalin:acetic acid:70% ethanol [1:1:18, v/v]) overnight under

vacuum (20 p.s.i.). Samples were dehydrated through a graded ethanol series and dried using a Tousimis Autosamdri-814 critical point dryer (Tousimis Research Corp., Rockville, MD). The samples then were mounted on stubs, coated with gold on a Cressington 108 sputter-coater (Cressington Scientific Instruments, Cranberry Township, PA), and observed using a Hitachi S-2500 scanning electron microscope (Tokyo, Japan).

Transmission Electron Microscopy

Tissue samples (2 mm^2) from leaves at developmental stages 1 to 5 were fixed in 2% glutaraldehyde in 0.05 M sodium cacodylate buffer, pH 6.9, overnight under vacuum (20 p.s.i.). Samples were washed in the same buffer and postfixed in 2.5% aqueous osmium tetroxide for 4 h at room temperature. Tissues were dehydrated in a graded ethanol series, infiltrated through ethanol:Spurr resin mixtures, embedded in pure Spurr resin, and polymerized at 70°C for 9 h. Gold sections were cut on a Reichert-Jung ultramicrotome, collected onto formvar-coated grids, and stained with uranyl acetate and lead citrate. Observations were made using a Philips 201 transmission electron microscope (Eindhoven, The Netherlands).

Terminal Deoxynucleotidyl Transferase–Mediated dUTP Nick End Labeling Assay

Tissue pieces (5 mm^2) from leaves at developmental stages 1 to 5 were fixed in FAA for 2 h and washed in 70% ethanol. The terminal deoxynucleotidyl transferase–mediated dUTP nick end labeling (TUNEL) assay was performed according to the manufacturer's instructions (Roche Diagnostics, Mannheim, Germany), and nuclei were stained by incubating in 3% (w/v) propidium iodide for 2 min. Samples were observed with a Zeiss LSM 410 inverted confocal laser scanning microscope (Carl Zeiss Canada, Toronto, Ontario) fitted with the following configuration: excitation at 488 nm and emission at 515 nm for fluorescein isothiocyanate, and excitation at 543 nm and emission at 570 nm for propidium iodide. A negative control was performed without terminal deoxynucleotidyl transferase enzyme, and a positive control was performed with DNase1.

DNA Isolation and Electrophoresis

Genomic DNA was isolated from stages 2 to 5. Approximately 100 mg of leaf tissue for each treatment was frozen in liquid nitrogen immediately after sampling and ground with a mortar and pestle to a fine powder. Isolation of DNA was performed using a DNeasy Plant Mini Kit (Qiagen, Mississauga, Ontario, Canada) according to the manufacturer's instructions. To observe DNA fragmentation, samples (0.5 $\mu g \cdot mL^{-1} \cdot lane^{-1}$, final concentration) were run with a 100-bp ladder on a 1% ethidium bromide agarose gel at a constant 50 V.

Video Imaging of Cytoplasmic Streaming

Video imaging of cytoplasmic streaming of epidermal and mesophyll cells in stages 1 to 3 was performed using a Hamamatsu C2400-77 video camera and control unit (Universal Imaging Corp., Westchester, PA). Images were contrast enhanced using an Image-1 image processing and analysis system (Universal Imaging Corp.). Recordings were made with a Sanyo TLS 2000 time-lapse video cassette recorder (Sanyo, Chatsworth, CA). Video prints were taken using a Sony video graphic printer (UP-895MD; Sony, Tokyo, Japan). When replayed, images were sped up 12 times. Each experiment was repeated at least three times for tissues observed at each stage through the progression of perforation formation.

Upon request, materials integral to the findings presented in this publication will be made available in a timely manner to all investigators on similar terms for noncommercial research purposes. To obtain materials, please contact Nancy G. Dengler, dengler@botany.utoronto.ca.

ACKNOWLEDGMENTS

We thank Michele Heath for help in videotaping cytoplasmic streaming and critical reading of the manuscript, Ronald Dengler for photography, Julie Kang, Kathy Sault, Sophie Nguyen, and Namiesh Seth for technical assistance, and Pauline Wang, Christine Robson, and Greg Vanlerberghe for help with agarose gel electrophoresis. We gratefully acknowledge the Natural Sciences and Engineering Research Council of Canada for a postdoctoral fellowship to A.H.L.A.N.G. and for Discovery Grants to J.S.G. and N.G.D.

Received August 8, 2003; accepted October 23, 2003.

REFERENCES

Beers, E.P. (1997). Programmed cell death during plant growth and development. Cell Death Differ. **4,** 649–661.

Calderon-Urrea, A., and Dellaporta, S. (1999). Cell death and cell protection genes determine the fate of pistils in maize. Development **126,** 435–441.

Campbell, R., and Drew, M.C. (1983). Electron microscopy of gas space (aerenchyma) formation in adventitious roots of *Zea mays* L. subjected to oxygen shortage. Planta **157,** 350–357.

Cheng, P.C., Greyson, R.I., and Walden, D.B. (1983). Organ initiation and the development of unisexual flowers in the tassel and ear of *Zea mays*. Am. J. Bot. **70,** 450–462.

Dellaporta, S.L., and Calderon-Urrea, A. (1994). The sex determination process in maize. Science **266,** 1501–1505.

Demura, T., et al. (2002). Visualization by comprehensive microarray analysis of gene expression programs during transdifferentiation of mesophyll cells into xylem cells. Proc. Natl. Acad. Sci. USA **99,** 15794–15799.

Dengler, N., and Tsukaya, H. (2001). Leaf morphogenesis in dicotyledons: Current issues. Int. J. Plant Sci. **162,** 459–464.

Dominguez, F., Moreno, J., and Cejudo, F.J. (2001). The nucleus degenerates by a process of programmed cell death during the early stages of wheat grain development. Planta **213,** 352–360.

Fath, A., Bethke, P.C., and Jones, R.L. (1999). Barley aleurone cell death is not apoptotic: Characterization of nuclease activities and DNA degradation. Plant J. **20,** 305–315.

Fukuda, H. (2000). Programmed cell death of tracheary elements as a paradigm in plants. Plant Mol. Biol. **44,** 245–253.

Giuliani, C., Consonni, G., Gavazzi, G., Colombo, M., and Dolfini, S. (2002). Programmed cell death during embryogenesis in maize. Ann. Bot. **90,** 287–292.

Gleissberg, S. (2002). Comparative developmental and molecular genetic aspects of leaf dissection. In Developmental Genetics and Plant Evolution, Q.C.B. Cronk, R.M. Bateman, and J.A. Hawkins, eds (London: Taylor & Francis), pp. 404–417.

Greenberg, J.T. (1996). Programmed cell death: A way of life for plants. Proc. Natl. Acad. Sci. USA **93,** 12094–12097.

Groover, A., DeWitt, N., Heidel, A., and Jones, A. (1997). Programmed cell death of plant tracheary elements differentiating in vitro. Protoplasma **196,** 197–211.

Grotewold, L., and Rüther, U. (2002). The Wnt antagonist Dickkopf-1 is regulated by Bmp signaling and c-Jun and modulates programmed cell death. EMBO J. **21,** 966–975.

Gunawardena, A.H.L.A.N., Pearce, D.M., Jackson, M.B., Hawes,

C.R., and Evans, D.E. (2001a). Characterization of programmed cell death during aerenchyma formation induced by ethylene or hypoxia in roots of maize (*Zea mays* L.). Planta **212,** 205–214.

Gunawardena, A.H.L.A.N., Pearce, D.M., Jackson, M.B., Hawes, C.R., and Evans, D.E. (2001b). Rapid changes in cell wall pectic polysaccharides are closely associated with early stages of aerenchyma formation, a spatially localized form of programmed cell death in roots of maize promoted by ethylene. Plant Cell Environ. **24,** 1369–1375.

He, C.J., Drew, M.C., and Morgan, P.W. (1994). Induction of enzymes associated with lysigenous aerenchyma formation in roots of *Zea mays* during hypoxia or nitrogen starvation. Plant Physiol. **105,** 861–865.

He, X., and Kermode, A.R. (2003). Nuclease activities and DNA fragmentation during programmed cell death of megagametophyte cells of white spruce (*Picea glauca*) seeds. Plant Mol. Biol. **51,** 509–521.

Heath, M.C. (2000). Hypersensitive response-related death. Plant Mol. Biol. **44,** 321–334.

Hoeberichts, F.A., and Woltering, E.J. (2002). Multiple mediators of plant programmed cell death: Interplay of conserved cell death mechanisms and plant-specific regulators. Bioessays **25,** 47–57.

Houot, V., Etienne, P., Petitot, A.S., Barbier, S., Blein, J.P., and Suty, L. (2001). Hydrogen peroxide induces programmed cell death features in cultured tobacco BY-2 cells, in a dose-dependent manner. J. Exp. Bot. **52,** 1721–1730.

Ito, J., and Fukuda, H. (2002). ZEN1 is a key enzyme in the degradation of nuclear DNA during programmed cell death of tracheary elements. Plant Cell **14,** 3201–3211.

Jacobson, M.D., Well, M., and Raff, M. (1997). Programmed cell death in animal development. Cell **88,** 347–354.

Jones, A.M. (2000). Does the plant mitochondrion integrate cellular stress and regulate programmed cell death? Trends Plant Sci. **5,** 225–230.

Jones, A.M. (2001). Programmed cell death in development and defense. Plant Physiol. **125,** 94–97.

Jones, A.M., and Dangl, J.L. (1996). Logjam at the Styx: Programmed cell death in plants. Trends Plant Sci. **1,** 114–119.

Kaplan, D.R. (1984). Alternative modes of organogenesis in higher plants. In Contemporary Problems in Plant Anatomy, R.A. White and W.C. Dickison, eds (New York: Academic Press), pp. 261–300.

Kozela, C., and Regan, S. (2003). How plants make tubes. Trends Plant Sci. **8,** 159–164.

Kuo, A., Cappelluti, S., Cervantes-Cervantes, M., Rodriguez, M., and Bush, D.S. (1996). Okadaic acid, a protein phosphatase inhibitor, blocks calcium changes, gene expression and cell death induced by gibberellin in wheat aleurone cells. Plant Cell **8,** 259–269.

Kuriyama, H. (1999). Loss of tonoplast integrity programmed in tracheary element differentiation. Plant Physiol. **121,** 763–774.

Kuriyama, H., and Fukuda, H. (2002). Developmental programmed cell death in plants. Curr. Opin. Plant Biol. **5,** 568–573.

Levine, A., Pennell, R.I., Alvarez, M.E., Palmer, R., and Lamb, C. (1996). Calcium-mediated apoptosis in a plant hypersensitive disease resistance response. Curr. Biol. **6,** 427–437.

Madison, M. (1977). A revision of *Monstera* (Araceae). Contrib. Gray Herb. Harv. Univ. **207,** 3–100.

Melville, R., and Wrigley, F.A. (1969). Fenestration in the leaves of *Monstera* and its bearing on the morphogenesis and colour patterns of leaves. Bot. J. Linn. Soc. **62,** 1–16.

Milioni, D., Sado, P., Stacey, N.J., Roberts, K., and McCann, M.C. (2002). Early gene expression associated with the commitment and differentiation of a plant tracheary element is revealed by cDNA-amplified fragment length polymorphism analysis. Plant Cell **14,** 2813–2824.

Mittler, R., and Lam, E. (1995). In situ detection of nDNA fragmentation during the differentiation of tracheary elements in higher plants. Plant Physiol. **108,** 489–493.

Mittler, R., and Lam, E. (1997). Characterization of nuclease activities and DNA fragmentation induced upon hypersensitive response cell death and mechanical stress. Plant Mol. Biol. **34,** 209–221.

Mittler, R., Simon, L., and Lam, E. (1997). Pathogen-induced programmed cell death in tobacco. J. Cell Sci. **110,** 1333–1344.

Nakashima, J., Takabe, K., Fujita, M., and Fukuda, H. (2000). Autolysis during in vitro tracheary element differentiation: Formation and location of the perforation. Plant Cell Physiol. **4,** 1267–1271.

Nelson, T., and Dengler, N. (1997). Leaf vascular pattern formation. Plant Cell **9,** 1121–1135.

Obara, K., Kuriyama, H., and Fukuda, H. (2001). Direct evidence of active and rapid nuclear degradation triggered by vacuole rupture during programmed cell death in Zinnia. Plant Physiol. **125,** 615–626.

Oberhammer, F., Wilson, J.W., Dive, C., Morris, I.D., Hickman, J.A., Wakeling, A.E., Walker, P.R., and Sikorska, M. (1993). Apoptotic death in epithelial cells: Cleavage of DNA to 300 and/or 50kb fragments prior or in the absence of internucleosomal fragmentation. EMBO J. **12,** 3679–3684.

Pennell, R.I., and Lamb, C. (1997). Programmed cell death in plants. Plant Cell **9,** 1157–1168.

Ryerson, D.E., and Heath, M.C. (1996). Cleavage of nuclear DNA into oligonucleosomal fragments during cell death induced by fungal infection or by abiotic treatments. Plant Cell **8,** 393–402.

Sculthorpe, C.D. (1967). The Biology of Aquatic Vascular Plants. (London: Edward Arnold Publishers).

Sergueff, M. (1907). Contribution á la Morphologie et la Biologie des Aponogetonacèes. PhD dissertation (Geneva: University of Geneva).

Simeonova, E., Sikora, A., Charzynska, M., and Mostowska, A. (2000). Aspects of programmed cell death during leaf senescence of mono- and dicotyledonous plants. Protoplasma **214,** 93–101.

Sinha, N. (1999). Leaf development in angiosperms. Annu. Rev. Plant Physiol. Plant Mol. Biol. **50,** 419–446.

Sugiyama, M., Ito, J., Aoyagi, S., and Fukuda, H. (2000). Endonucleases. Plant Mol. Biol. **44,** 387–397.

Thomas, H., Ougham, H.J., Wagstaff, C., and Stead, A.D. (2003). Defining senescence and death. J. Exp. Bot. **54,** 1127–1132.

Tomlinson, P.B. (1982). Aponogetonaceae: Family descriptions. In Anatomy of the Monocotyledons. VII. Helobiae (Alismatideae), C.R. Melcalfe, ed (Oxford, UK: Clarendon Press), pp. 198–225.

Trècul, A. (1854). Notes sur la formation des perforations que present les feuilles de quelque Aroidèes. Ann. Sci. Nat. Ser. Bot. **1,** 37–40.

Wang, M., Hoekstra, S., Bergen, S., Lamers, G.E.M., Oppedijk, B.J., Heijden, M.W., Priester, W., and Schilperoort, R.B. (1999). Apoptosis in developing anthers and the role of ABA in this process during androgenesis in *Hordeum vulgare* L. Plant Mol. Biol. **39,** 489–501.

Wang, M., Oppedijk, B.J., Lu, X., Duijin, B.A., and Schilperoort, R.A. (1996). Apoptosis in barley aleurone during germination and its inhibition by abscisic acid. Plant Mol. Biol. **32,** 1125–1134.

Wyllie, A.H., Kerr, J.F.R., and Currie, A.R. (1980). Cell death: The significance of apoptosis. Int. Rev. Cytol. **68,** 251–306.

Young, T.E., Gallie, D.R., and DeMason, D.A. (1997). Ethylene-mediated programmed cell death during maize endosperm development of wild-type and *shrunken2* genotypes. Plant Physiol. **115,** 737–751.